International Journal of Pharmaceutics, 14 (1983) 313–323
Elsevier Biomedical Press

Dissolution at porous interfaces III. Pore effects in relation to the hydrodynamics at a rotating disc surface

H. Grijseels *, D.J.A. Crommelin and C.J. de Blaey **

Department of Pharmaceutics, Subfaculty of Pharmacy, University of Utrecht, Catharijnesingel 60, 3511 GH Utrecht (The Netherlands)

(Received September 1st, 1982)
(Accepted October 13th, 1982)

Summary

The dissolution rate-increasing effect of pores drilled into a dissolving tablet surface was studied in a rotating disc apparatus. The increase of the dissolution rate due to one pore, ΔR, was measured as a function of the pore diameter, the pore position and the rotation speed of the tablet surface.

From the obtained results the critical pore diameters were determined. They appeared to be inversely proportional to the friction velocity at the surface, a hydrodynamic variable dependent both on the radial position on the surface and on the rotation speed. In addition, ΔR was found to be related to the friction velocity on the one hand and to the extent the pore size exceeds the critical pore diameter on the other.

Introduction

It has been shown in previous papers (Grijseels and de Blaey, 1981; Grijseels et al., 1983) that pores in a tablet surface increase the dissolution rate of that surface. The diameter of a drilled pore had to exceed a critical value to bring about this rise in dissolution rate. Other conclusions from previous experiments (Grijseels et al., 1983) were: (1) the increase in dissolution rate is a consequence of the disturbing effect of a pore on the hydrodynamics at the solid/liquid interface; (2) when the

* Present address: Cedona Pharmaceuticals B.V., P.O. Box 850, 2003 RW Haarlem, The Netherlands.
** To whom correspondence should be addressed.

0378-5173/83/0000–0000/$03.00

hydrodynamic variables (rotation speed, dissolution medium, pore shape and pore position) are kept constant, the critical pore diameter is the same for all the substances investigated; (3) the increase of the dissolution rate is directly related to the solubility and the effective diffusion coefficient of the dissolving solid; and (4) the diameter of a cylindrical pore is the dominant geometric variable provided the depth : diameter ratio of the pore exceeds a value of about 1.5.

The purpose of this paper is to describe the influence of some hydrodynamic factors on the dissolution rate of the tablet surface more quantitatively. The effect of rotation speed, pore diameter and position of the pore in the surface are investigated in a rotating disc set-up.

Theoretical

In a previous paper (Grijseels et al., 1981) it has been explained that near the surface of a rotating disc a hydrodynamic boundary layer develops as a direct consequence of the friction that occurs when a viscous fluid flows along a solid surface. An extension of the theoretical background is given here which will make it possible to link our results with similar experimental work performed in electrochemistry. The drag acting on the surface of a rotating disc is known as the local parietal friction or shear stress, τ. Actually τ is the flux of momentum transferred between the flowing liquid and the wall and is defined as

$$\tau = \nu \cdot \rho \cdot \frac{du}{dy} \tag{1}$$

where u denotes the fluid velocity parallel to the surface (other symbols are listed in the appendix). A derived variable is the friction velocity, v_f, which is a function of τ and the fluid density, ρ,

$$v_f = \left(\frac{\tau}{\rho}\right)^{1/2} = \left(\nu \cdot \frac{du}{dy}\right)^{1/2} \tag{2}$$

v_f can be considered as a characteristic value for the average velocity in the boundary layer. In a laminar flow regimen at a rotating disc the friction velocity is given by (Schlichting, 1968; Deslouis et al., 1980):

$$v_f = 0.89 \cdot \frac{\nu}{r} \cdot Re^{3/4} = 0.89 \cdot \nu^{1/4} \cdot r^{1/2} \cdot \omega^{3/4} \tag{3}$$

Eqn. 3 implies that the friction velocity depends on the radial position on the disc surface as well as on the angular velocity of the disc.

Concerning a smooth surface it is known that the laminar flow pattern changes into a turbulent regimen above a critical Reynolds number. Deslouis et al. (1980) determined for the friction velocity in turbulent flow at a rotating disc:

$$v_f = 0.17 \cdot \frac{\nu}{r} \cdot Re^{0.91} \tag{4}$$

In this case v_f has to be interpreted as the velocity of turbulence eddies at the border of the viscous sublayer (Levich, 1962).

Now we will treat first the influence of the above-mentioned hydrodynamic parameters on the mass transfer at a smooth rotating disc surface. Later we will focus on the corresponding process at a rough surface, to which out interest is directed in particular.

Mass transfer at a smooth surface

In case turbulence is absent or has a negligible effect within the diffusion boundary layer the mass flux, j, to or from a rotating disc is proportional to the cube-root of the parietal friction, τ (Aimeur et al., 1973; Deslouis et al., 1981). In combination with Eqn. 2 this leads to the relationship

$$j \sim (v_f)^{2/3} \tag{5}$$

This equation is valid if the surface is smooth and the Reynolds number is below 2×10^5, no turbulence being present.

On the other hand, the mass flux, j, in turbulent flow is directly proportional to v_f (Meklati and Daguenet, 1975; Deslouis et al., 1977):

$$j \sim v_f \tag{6}$$

So a sharp distinction can be made between laminar and turbulent flow conditions concerning the dependence of mass flux, j, on the friction velocity. A relationship between the mass flux, j, and the angular velocity of the disc, ω, can be derived for different flow regimens.

For laminar flow, one obtains from Eqns. 3 and 5

$$j \sim \omega^{1/2} \tag{7}$$

The validity of this relationship was verified for both the entire disc surface and microelectrodes embedded in such a surface (Deslouis et al., 1980; 1981).

Turbulent conditions imply the combination of Eqns. 4 and 6:

$$j \sim \omega^{0.91} \tag{8}$$

The exponent in Eqn. 8 was predicted theoretically by Levich (1962) and confirmed experimentally by Deslouis et al. (1980). But in contrast with the laminar flow situation, j depends also on the radial coordinate, r.

Mass transfer at a rough surface

One of the assumptions on which Levich (1962) based his theoretical derivations is that the rotating disc has a perfectly smooth surface, since roughness causes a considerable decrease in the value of the critical Reynolds number above which turbulence occurs. The critical height, i.e. the height which just does not provoke transition to turbulent flow, of a single, cylindrical roughness element is given by

(Schlichting, 1968):

$$\frac{v_f \cdot h_{crit}}{\nu} = 7 \tag{9}$$

Here v_f denotes the friction velocity at the wall in the laminar boundary layer at the position of the roughness element. The characteristic value in Eqn. 9 applies to measurements performed with a circular wire attached to a wall. For sharp elements considerably smaller values are found (Schlichting, 1968; Levich, 1962).

Uniform rough surfaces were investigated in a large number of studies (Theodorsen and Regier, 1944; Meklati and Daguenet, 1973, 1975; Mollet and Daguenet, 1981). Due to protrusions and depressions at such a surface even at low rotation speeds, a turbulent flow regimen can develop with a character different from turbulence near a smooth surface at high Reynolds numbers. When the roughness elements are large with respect to the thickness of the laminar boundary layer, separation already occurs at low rotation speeds resulting in turbulence in the wake of the obstacles. Theodorsen and Regier (1944) glued coarse sand (0.25 mm) to a surface and found a value of 3.3 for the relationship in Eqn. 9. Dorfman (1958) found experimentally a relationship between the friction velocity at a uniform rough surface and the roughness dimension h:

$$v_f \approx 0.136 \cdot r \cdot \omega \cdot (1 + \alpha^2) \cdot \left(\frac{h}{r}\right)^{0.133} \tag{10}$$

where $\alpha \approx 0.512 \cdot \left(\frac{h}{r}\right)^{0.043}$

In the present study we investigated the influence of single, cylindrical pores on the dissolution rate of a rotating disc surface. Referring to the considerations mentioned above, based both on theory and experiments, we try to relate quantitatively measurable pore effects (e.g. the critical pore diameter) to hydrodynamic variables like the friction velocity.

Materials and methods

Disodium tetraborate decahydrate (borax, Ph. Eur.) was used as the test material. The procedures for manufacturing the borax pellets and drilling pores are described earlier (Grijseels and de Blaey, 1981). The pores were drilled in such a geometric configuration that they formed a 'fairy ring' around the centre of the tablet surface. The radius of this ring was 2.5 mm (henceforth called: centre position) or 5.0 mm (edge position) with a tablet radius of 7.5 mm. Per tablet 2, 4 or 8 pores were drilled in proportion to their diameter and position.

In this study the diameters of the cylindrically shaped pores ranged from 0.10 to 2.00 mm. In pursuance of previous experiments where the influence of the pore

depth was examined (Grijseels et al., 1983), the pores were drilled to a depth that exceeded their diameter with about 1 mm.

The rotating disc set-up and the practical execution of the dissolution rate measurements are described earlier (Grijseels et al., 1983). Experiments were performed at 5 rotation speeds ranging from 70 ± 0.5 rpm up to 340 ± 2 rpm. Each experiment was done at least in triplicate to allow further statistical computations.

Results and discussion

Fig. 1 shows the dissolution rate values of tablet surfaces as a function of the square-root of the angular velocity. In agreement with Eqn. 7, the data for intact tablet surfaces lay on a straight line (lower-most line in Fig. 1a). The tablets provided with pores produce straight lines too when the data are plotted in this way, but they are steeper (Student's t-test; $P = 0.95$) than the line representing the intact

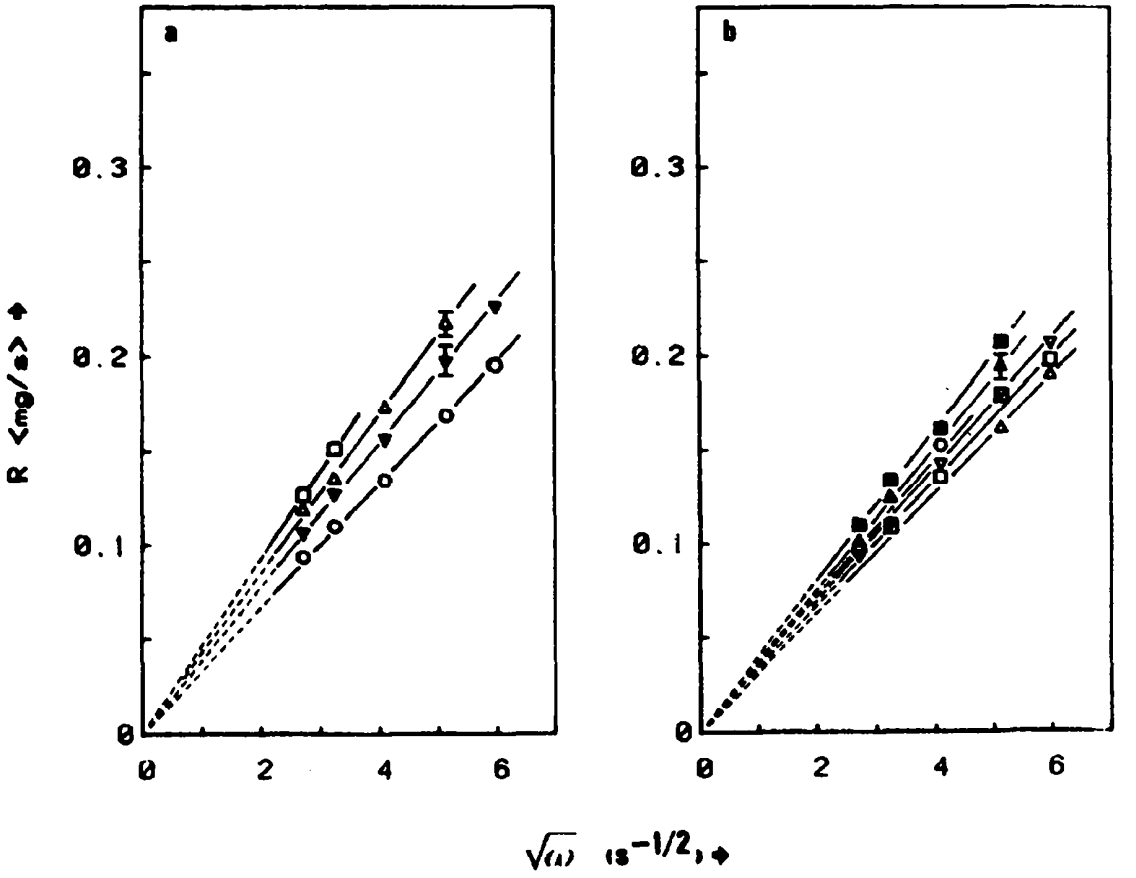

Fig. 1. Influence of the rotation speed on the dissolution rate of borax tablets provided with four (a) or eight (b) pores of varying diameter in the edge position (pore axis 5.0 mm from the centre of the pellet surface). (a) □, pore diameter 2.00 mm; △, 1.50 mm; ▽, 1.00 mm; ○, surface without pores. (b) ■, 0.70 mm; ▲, 0.50 mm; ○, 0.40 mm; ▽, 0.30 mm; □, 0.20 mm; △, 0.10 mm. Vertical bars represent the standard deviation. If not shown the standard deviation fell within the drawn symbol.

surface. It can be concluded from Fig. 1 that pores cause a rise in the dissolution rate of the surface and that the extent to which the pore increases R is related both to the rotation speed of the disc and to the pore diameter.

Another way to interpret the same data was achieved by calculating the increase of the dissolution rate per pore, ΔR. All the computed values of ΔR, for both the centre and the edge position, are collected in Table 1. Part of these data, viz. the results of 5 rotation speeds with pores in the edge position, are shown in Fig. 2. By analogy with earlier observations (Grijseels and de Blaey, 1981; Grijseels et al., 1982), these lines are straight and their slopes increase with the rotation speed. An advantage of plotting our results in this way is that we can find the critical pore diameter as the intersection of the abscissa and the extrapolated regression lines. By means of linear regression calculations we obtained the values of d_{crit} together with their standard deviations for both the edge and the centre position. The results are summarized in Table 2. If we assume that it is allowed to replace h_{crit} in Eqn. 9 by the equivalent d_{crit}, the latter should be inversely proportional to the local friction velocity. In Table 2 the relevant values of v_f, calculated by means of Eqn. 3, are

TABLE 1

INCREASE OF THE DISSOLUTION RATE PER PORE, ΔR, AS A FUNCTION OF THE ROTATION SPEED, THE PORE DIAMETER AND THE PORE POSITION (EDGE = PORE AXIS 2.5 mm FROM THE SURFACE EDGE; CENTRE = PORE AXIS 5.0 mm FROM THE SURFACE EDGE)

Pore diameter (mm)	rpm 70	100	160	250	340
	ω 7.33	10.47	16.76	26.18	35.60
Edge					
0.10	–	–	–	−0.69 (0.23)	−0.06 (0.13)
0.20	–	−0.13 (0.06)	0.15 (0.15)	1.31 (0.15)	0.98 (0.13)
0.30	0.06 (0.09)	0.20 (0.07)	1.06 (0.13)	1.59 (0.12)	2.18 (0.15)
0.40	0.31 (0.11)	–	1.79 (0.19)	–	–
0.50	0.87 (0.11)	1.78 (0.06)	2.19 (0.22)	3.22 (0.18)	3.75 (0.19)
0.70	2.03 (0.09)	2.96 (0.07)	3.37 (0.20)	4.91 (0.16)	6.42 (0.28)
1.00	3.23 (0.23)	4.39 (0.07)	5.52 (0.40)	7.37 (0.42)	9.14 (0.29)
1.50	6.13 (0.28)	6.95 (0.16)	9.54 (0.14)	12.22 (0.34)	–
2.00	8.27 (0.23)	10.46 (0.41)	–	–	–
Centre					
0.10	–	–	–	−0.64 (0.20)	−0.29 (0.11)
0.20	–	−0.03 (0.06)	−0.03 (0.17)	0.25 (0.17)	0.61 (0.14)
0.30	–	0.28 (0.07)	0.61 (0.13)	0.69 (0.20)	1.28 (0.10)
0.50	–	1.13 (0.07)	1.27 (0.33)	1.71 (0.42)	2.55 (0.19)
0.70	–	2.10 (0.12)	2.71 (0.28)	2.79 (0.46)	4.39 (0.19)
1.00	–	3.46 (0.18)	4.08 (0.29)	4.04 (0.92)	7.01 (0.38)
1.50	–	5.09 (0.31)	6.20 (0.63)	6.61 (0.67)	–
2.00	–	7.41 (0.49)	–	–	–

ΔR is expressed in $\mu g \cdot s^{-1}$, between brackets the standard deviation. These values and standard deviations are computed from the data in Fig. 1 and the corresponding data of pores in the centre position. – = no experimental data available.

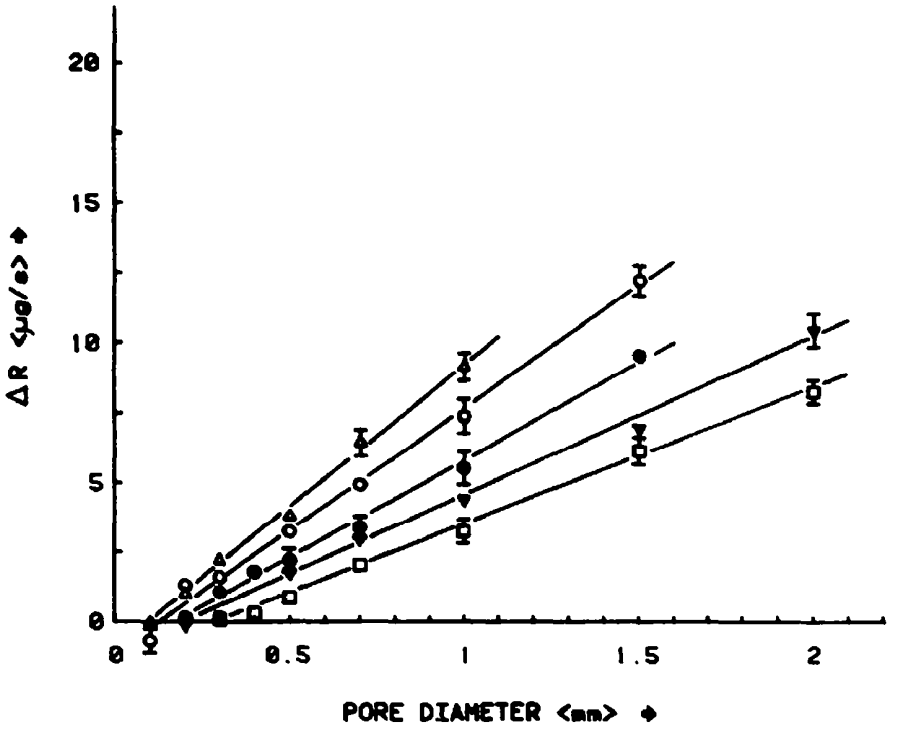

Fig. 2. Increase of the dissolution rate per pore (ΔR) as a function of the diameter of pores in the edge position. △, 340 rpm; ○, 250 rpm; ●, 160 rpm; ▼, 100 rpm; □, 70 rpm. Vertical bars represent standard deviation. If not shown the standard deviation fell within the drawn symbol.

collected. We plotted in Fig. 3 d_{crit} as a function of the reciprocal of v_f. Except for some deviating points, a linear correlation seems to exist. Using the underlined data in Table 2, we determined from least-squares regression analysis:

$$\frac{v_f \cdot d_{crit}}{\nu} = 2.7 \text{ (S.D. } = 0.1)$$

TABLE 2

VALUES OF THE FRICTION VELOCITY COMPUTED BY MEANS OF EQN. 3 AND THE CRITICAL PORE DIAMETER CALCULATED FROM THE DATA IN TABLE 1

rpm	Edge		Centre	
	v_f ($mm \cdot s^{-1}$)	d_{crit} (mm)	v_f ($mm \cdot s^{-1}$)	d_{crit} (mm)
70	8.9	0.31 (0.03)	–	–
100	11.6	0.23 (0.04)	8.2	0.21 (0.03)
160	16.6	0.18 (0.03)	11.7	0.19 (0.04)
250	23.1	0.13 (0.02)	16.4	0.17 (0.03)
340	29.1	0.10 (0.02)	20.6	0.14 (0.02)

Between brackets is given the standard deviation. – = not available.

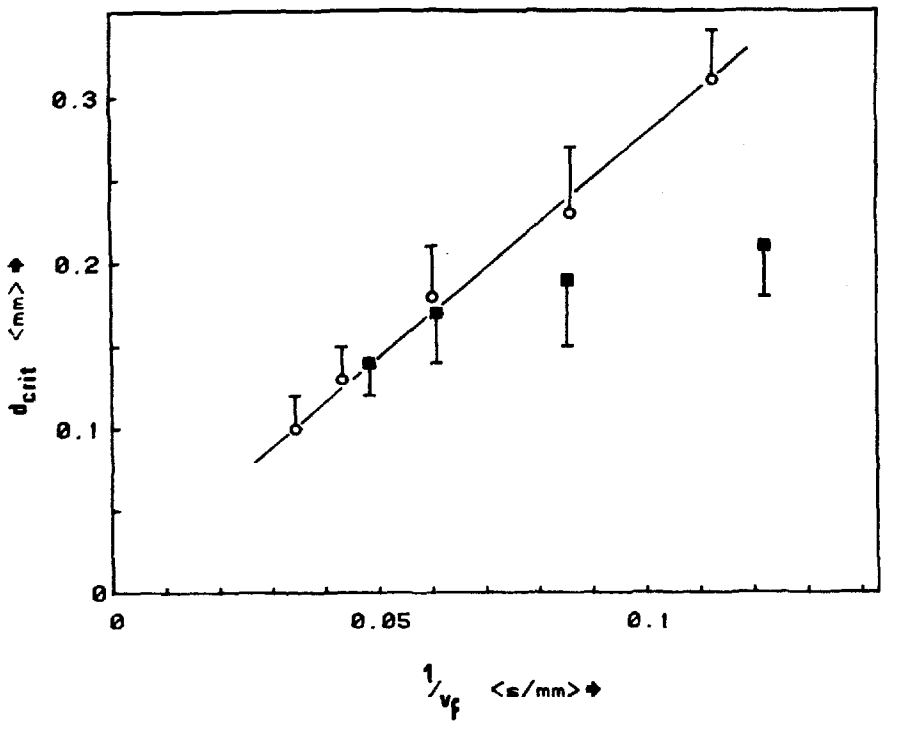

Fig. 3. Plot of the critical pore diameter versus the reciprocal of the friction velocity. ○, edge position; ■, centre position. Vertical bars represent the standard deviation.

Although this value is considerably lower than the one mentioned in Eqn. 9 for a wire attached to a wall, it is not surprising that a sharp-edged cylindrical pore gives faster rise to turbulence than a streamlined circular wire with its axis parallel to the surface.

Two points in Fig. 3 do not satisfy the predicted and observed relationship. They represent pores in the centre position at the lower rotation speeds of 100 and 160 rpm. An explanation for their deviating behaviour can be found in the fact that these pores lay within a central zone on the rotating disc surface where $Re < 100$. As we mentioned in a previous paper (Grijseels et al., 1983), within this central portion of the surface the thickness of the hydrodynamic boundary layer is *not* independent of the radial distance from the centre and therefore it is questionable whether in this area Eqn. 3 can be used correctly to calculate the friction velocity.

Returning to the results in Fig. 2 it is obvious that the increase in dissolution rate due to the presence of a pore in the dissolving surface is related both to the rotation speed of the surface and to the pore size. Clearly for all rotation velocities investigated a direct proportionality exists between ΔR and the pore diameter from the critical pore size upwards, which can be expressed in the form

$$\Delta R \sim (d - d_{crit}) \tag{11}$$

The increase in dissolution rate, ΔR, is caused by turbulence effects arising down-

stream the leading edge of the pore. The local Reynolds number in the wake behind the pore increases as the fluid flows towards the edge of the rotating disc surface. Therefore it is unlikely that the turbulence will be dampened like we noticed in the centrifugal stirrer apparatus (Grijseels and de Blaey, 1981). This implies that the turbulence developing in the wake of the pore extends not only over the dissolving surface of the tablet but also over the surface of the perspex holder we used during our experiments. Of course the increase in dissolution rate involved only takes place at the pellet surface. So the shorter the distance the fluid has to cover from the pore to the edge of the tablet, the smaller is the part of the pellet surface exposed to the dissolution rate-promoting effect of the turbulent wake. The length of the trough behind a pore decreases both with increasing rotation speed and with increasing distance between pore and surface centre, thus with increasing v_f. So the friction velocity at the leading edge of a pore has two opposing effects on the erosion process of the tablet surface in the wake of the pore. On the one hand ΔR increases with increasing v_f due to the higher intensity of turbulence. On the other hand v_f has a negative influence on the length of the erosion trough behind the pore. These considerations lead us to the assumption that a relationship exists of the form

$$\Delta R \sim (v_f)^p \tag{12}$$

Combining the relationships expressed in Eqn. 11 and Eqn. 12 we can write finally

$$\Delta R = k \cdot (v_f)^p \cdot (d - d_{crit}) \tag{13}$$

Eqn. 13 implies that the increase in dissolution rate depends in the first place on the local friction velocity, that is the characteristic velocity in the boundary layer at the leading edge of a pore which is determined by the position of the pore and the revolution speed of the disc surface. Secondly ΔR is related to the extent the pore size exceeds the critical pore diameter. We concluded from the data in Table 2 that d_{crit} itself is a function of v_f too. Using the empirical relationship we found in Fig. 3, viz. $d_{crit} = 2.7/v_f$, it was possible to calculate for all pore diameters, pore positions and rotation speeds collected in Table 1 the corresponding values of v_f and $(d - d_{crit})$. By applying linear regression analysis to a log–log plot of $\Delta R/(d - d_{crit})$ versus v_f the magnitude of exponent p in Eqn. 13 was found to be 0.53 (S.D. = 0.07). Fig. 4 shows all data plotted according to Eqn. 13 using for p a value of 0.5. The good correlation that is found between both variables ($r = 0.988$) confirms the proposed model of the dissolution rate-promoting effect of pores in a rotating disc surface.

The results presented here can be summarized as follows: (1) large pores in a tablet surface provoke turbulence associated with an enhanced dissolution rate of the surface downstream the pore; (2) this increase is observed only when the pore diameter exceeds a critical value, which appears to be inversely proportional to the friction velocity in the boundary layer; and (3) the increase of the dissolution rate due to a pore in a rotating disc surface appears to be directly proportional to the difference in actual and critical pore diameter and to the square-root of the friction velocity at the leading edge of the pore.

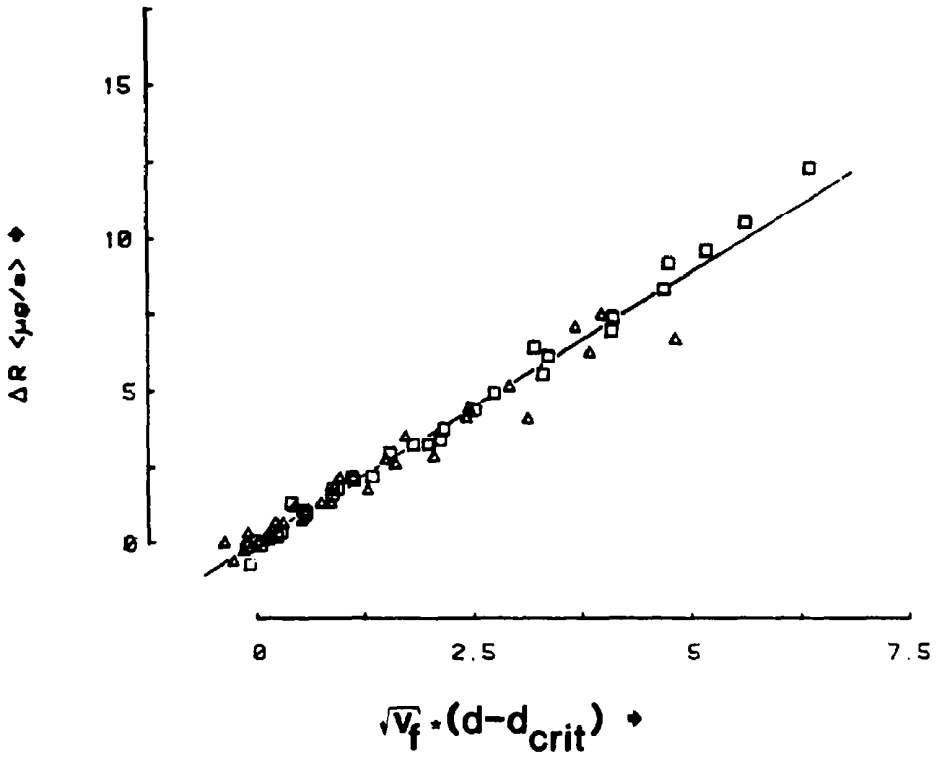

Fig. 4. Increase of the dissolution rate per pore (ΔR) versus the difference of the actual and critical pore diameter times the square-root of the local friction velocity. □, edge position; △, centre position. The drawn line is computed by linear regression analysis.

Acknowledgement

The authors are indebted to Mr. L. van Bloois who performed the experiments for the major part.

Abbreviations

d	pore diameter	(m)
d_{crit}	critical pore diameter	(m)
h	size of roughness	(m)
h_{crit}	critical height of a protrusion	(m)
j	mass flux	$(kg \cdot m^{-2} \cdot s^{-1})$
k	constant	
P	probability	
p	exponent in Eqn. 12 and 13	
r	radial coordinate	(m)
R	dissolution rate	$(kg \cdot s^{-1})$
ΔR	increase of R due to one pore	$(kg \cdot s^{-1})$

Re	Reynolds number ($= r^2 \cdot \omega \cdot \nu^{-1}$)	
S.D.	standard deviation	
u	fluid velocity parallel to the surface	$(m \cdot s^{-1})$
v_f	friction velocity	$(m \cdot s^{-1})$
y	distance normal to the surface	(m)
α	cf. Eqn. 10	
ν	kinematic viscosity	$(m^2 \cdot s^{-1})$
ρ	fluid density	$(kg \cdot m^{-3})$
τ	parietal friction (shear stress)	$(kg \cdot m^{-1} \cdot s^{-2})$
ω	angular velocity	(s^{-1})

References

Aimeur, F., Daguenet, M., Kermiche, F. and Meklati, M., Theorie et applications des microelectrodes. Electrochim. Acta, 18 (1973) 87–93.

Deslouis, C., Epelborn, I., Keddam, M., Viet, L., Dossenbach, O. and Ibl, N., Recent progress in the methodology of the rotating disk electrode. In Spalding, D.B. (Ed.), Physicochemical Hydrodynamics, Advance Publications, London, 1977, Part 2, pp. 939–971.

Deslouis, C., Tribollet, B. and Viet, L., Local and overall mass transfer rates to a rotating disk in turbulent and transition flows. Electrochim. Acta, 25 (1980) 1027–1032.

Deslouis, C., Gabrielli, C. and Tribollet, B., Multi-channel potentiostatic control in electrochemistry: localised mass-transfer rates at the rotating disc electrode. Physico-Chemical Hydrodyn., 2 (1981) 23–30.

Dorfman, L.A., Drag of a rotating rough disc (English translation). Zh. Tekh. Fiz., 28 (1958) 280–286.

Grijseels, H., Crommelin, D.J.A. and de Blaey, C.J., Hydrodynamic approach to dissolution rate. Pharm. Weekbl. Sci. Edn., 3 (1981) 129–144.

Grijseels, H. and de Blaey, C.J., Dissolution at porous interfaces. Int. J. Pharm., 9 (1981) 337–347.

Grijseels, H., van Bloois, L., Crommelin, D.J.A. and de Blaey, C.J., Dissolution at porous interfaces II. A study of pore effects through rotating disc experiments. Int. J. Pharm., 14 (1983) 299–311.

Levich, V.G., Physicochemical Hydrodynamics, Prentice Hall, New Jersey, 1962, pp. 1–184.

Meklati, M. and Daguenet, M., Etude expérimentale du courant limite de diffusion turbulente sur une électrode à disque tournant rugueuse. J. Chim. Phys. 70 (1973) 1102–1106.

Meklati, M. and Daguenet, M., Etude de la diffusion turbulente sur des surfaces lisses et rugueuses dans un liquide de Newton et d'Ostwald. J. Chim. Phys., 72 (1975) 262–264.

Mollet, L. and Daguenet, M., Etude expérimentale des courantes limites de diffusion sur des électrodes rugueuses à disques tournants. J. Chim. Phys., 78 (1981) 61–66.

Schlichting, H., Boundary Layer Theory, McGraw-Hill, New York, 1968, pp. 94–99 and 511.

Theodorsen, T. and Regier, A., Experiments on drag on revolving disks, cylinders and streamline rods at high speeds. N.A.C.A. Rept. No. 793 (1944) 367–384.